Hybrid Beamforming for Nonlinear SWIPT in Terahertz Massive MIMO Systems

MD. ASIF HOSSAIN
Department of Electrical and Electronic Engineering
Southeast University
Tejgaon, Dhaka-1208,
BANGLADESH

Abstract: - Terahertz communications are one of the 6G technologies, offering very high data rates with an extremely large path loss and very short range, making it extremely challenging for energy-limited IoT devices. Simultaneous Wireless Information and Power Transfer (SWIPT) has emerged, but new designs employ an optimal linear energy-harvesting model that does not account for nonlinear rectifier operations. By contrast, we introduce a novel hybrid beamforming solution for wideband THz massive MIMO communications that incorporates a realistic nonlinear energy-harvesting model. We formulate an optimization problem to maximize a weighted sum of the rate and the total harvested energy, subject to transmit power constraints, constant-modulus constraints, and quality-of-service requirements. The derived nonconvex optimization problem can be efficiently addressed employing a two-stage solution. The first stage focuses on optimizing analog beamformers via shaping signals on the main Line-of-Sight components and addressing frequency-dependent beam squint effects. Digital precoders and coordinate-wise power splitting ratios will be jointly optimized with an efficient Successive Convex Approximation (SCA) method using Block Coordinate Descent (BCD). Simulation experiments demonstrate superior gains for the proposed solution compared with traditional designs that exploit optimal linear energy models, and these benefits will be more pronounced for near- and mid-field THz communications. Our work demonstrates an intrinsic trade-off in realistic THz communications and energy-limited IoT networking. These findings and challenges underscore the urgent need to model THz communications that consider RF circuit modules and to enable efficient, energy-saving 6G wireless networking for simultaneous wireless power and high-throughput communications.

Key-Words: - THz communication, Wireless Information and Power Transfer (SWIPT), energy harvesting, massive MIMO, Beamforming, Joint Optimization Problem, next-generation wireless communications, Block Coordinate Descent.

Received: April 21, 2025. Revised: August 19, 2025. Accepted: September 23, 2025. Published: December 31, 2025.

1 Introduction

The ever-increasing demand for data-intensive services from applications such as extended reality (XR), holographic communications, and very large-scale IoT networks [1] has driven the need for next-generation wireless communications beyond 5G. Terahertz communications spanning 0.1-10 THz have been identified as an enabler and essential component for next-generation 6G communications [2] because they offer unprecedented bandwidth, terabit-per-cond data rates, and low-latency communications [3] Nevertheless, due to THz signals' unique properties like high molecular absorption, high free space path loss, and very low diffraction, ranging and spanning within wireless communications becomes an issue and requires highly directional beamforming based on large-scale antennas. [4] Although these offer very high-rate data transmission capabilities, they are highly challenging for energy-restricted wireless devices with limited battery life [5].

To address these two challenges concurrently, Simultaneous Wireless Information and Power Transfer (SWIPT) has attracted growing interest in recent years as an essential technique for future wireless networks[6] As it jointly designs information and energy transfers using the same RF signal, SWIPT would enable wireless charging, eliminate the need for wired charging, and increase the lifespan of low-power wireless devices. As described before, traditional SWIPT systems separate the received signal using

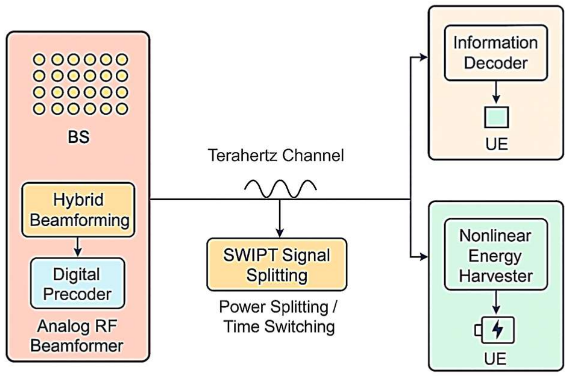

Fig. 1: Concept diagram of the paper, Source: created by the author.

either time switching (TS) or power splitting (PS) for information and energy reception, respectively [7]. Note that most existing SWIPT architectures have adopted a linear energy-harvesting (EH) model, which proportionally relates the received DC power to the signals at ratios [8]. Although it is more convenient and easier to process using mathematical analysis, it does not depict an energy-harvesting circuit with a low and a high region with respect to its sensitivity [9].

Recent research on EH models has shown that linear EH models can sometimes result in significant overestimation or underestimation of the actual harvested energy, leading to suboptimal resource allocation and significantly affecting system performance. [10] [11]. For example, in THz bands, the available transmit power is physically limited by hardware and regulatory constraints. Yet, the RF power received might drop below the energy rectifier threshold, leading to zero energy conversion for a strong information signal. [12]. On the other hand, at very short distances, it might result in an excessive energy wastage due to saturation at the energy rectifier. [13]. Hence, it is essential to integrate an appropriate, more pragmatic EH model, such as a sigmoid or piecewise-linear EH model.

Although nonlinear EH plays a very significant role, its implementation within THz communication systems has yet to be fully investigated. Additionally, THz massive MIMO systems usually adopt a hybrid A/D beamforming strategy. That strategy aims at optimizing hardware complexity, energy consumption, and spectral efficiency. [14][15]. Specifically, within these systems, a dedicated analog beamformer, implemented with phase shifters, manages beam angular directionality, while a digital baseband precoder enables concurrent transmission of multiple streams and interference mitigation. Nevertheless, extending these concepts to SWIPT requires simultaneous optimization of information and energy transport, which are clearly conflicting objectives. [16]. A good example here is maximum-rate transmission, which typically requires specific beams pointing to specific receivers, and efficient energy harvesting. [17], preferably with more extensive coverage. Yet, these challenges are made more difficult by a frequency-dependent beam squint phenomenon, caused by THz-wideband fading, in which pointing directions differ across subrriers, negatively impacting signal alignment and energy transport due to beam distortion. [18].

To address these problems, we propose a hybrid beamforming method for SWIPT in wideband THz massive MIMO communications, incorporating a realistic nonlinear EH model. Figure 1 illustrates the conceptual diagram for this research. Specifically, we focus on downlink transmission with a multi-antenna BS and multiple single-antenna receivers, including PS receivers. Our task is to co-design the analog and digital beamformers to maximize a weighted sum of spectral efficiency and total harvested energy, while satisfying transmit power constraints and CM constraints on the analog precoder. This formulation leads to a highly coupled, NP-hard optimization problem. To solve these problems effectively, we propose a two-stage algorithm. First, we propose an algorithm for designing the analog precoder based on the main LoS components of THz communications. Second, we optimize the digital beamformers using SCA. [19] techniques, accounting for the nonlinear EH model. We have considered the actual saturation and sensitivity aspects associated with rectifier designs for realistic performance analysis.

The key contribution made in this work can be listed as follows:

- We propose a holistic system model for THz massive MIMO based on SWIPT and taking into account various wideband effects, molecular absorption, and a nonlinear energy harvesting receiver model.
- We formulate a joint optimization problem of hybrid beamforming with consideration of information and energy transport, as well as hardware constraints.
- We propose an efficient technique for beamforming with two stages involving analog beam alignment with squint correction and digital precoding using SCA.

- Computer simulations have shown that the suggested approach clearly outperforms competing methods incorporating either linear EH or omitting beam squint effects in short- and mid-distance THz communications.

Although some very recent research efforts have addressed hybrid beamforming for THz SWIPT [15] [18] and nonlinear EH for mmWave communications [11] [13], respectively, a unified framework that considers broad beam squint effects, LoS-dominant analog designs, and sigmoid EH functions together with a unified optimization strategy for SWIPT remains uncharted. By contrast, our contribution represents the first work that: (i) integrates frequency-dependent squints with analog beamforming designs for SWIPT systems, and (ii) identifies the role of THz propagation and circuit nonlinearities on rate and energy trade-offs.

The remaining sections of this paper are structured as follows. Section 2 will introduce the system and channel models. Section 3 will discuss the nonlinear receiver and signal model. Section 4 will introduce the beamforming algorithm. And then there will be simulations and a conclusion in Sections 5 and 6.

2 System Model

We focus on a downlink THz massive MIMO system, with a BS with N_t antenna elements serving K single-antenna user devices. It will be assumed that each user device is capable of conducting SWIPT with a receiver employing a power-splitting technique. The BS will operate within the THz band, for instance, 140-200GHz, employing a hybrid analog and digital beamforming method that promotes strong directional gain and multi-user simultaneous transmission with a broad signal band. The goal will be to jointly optimize the beamformer design using an objective function that weights spectral efficiency and harvested energy.

2.1 THz Channel Model

The THz channel is characterized by high directionality, molecular absorption, and sparse multipath components. [20]. Due to the short wavelength, only a few dominant propagation paths exist, typically dominated by the line-of-sight (LoS) component. [21]. THz channel measurements well support this sparsity in indoor/short-range scenarios [20] [21], where the LoS path typically dominates by 15–20 dB over NLoS components. We adopt a narrowband cluster-based geometric channel model for each subcarrier, which can be extended to wideband scenarios via OFDM.

The channel vector between the BS and user k on subcarrier n is modeled as [22]:

$$\mathbf{h}_k[n] = \sqrt{\frac{N_t}{L_k}} \sum_{\ell=1}^{L_k} \beta_{k,\ell}[n] \mathbf{a}\left(\phi_{k,\ell}, \theta_{k,\ell}\right), \tag{1}$$

where:

- L_k is the number of propagation paths for user k,
- $\beta_{k,\ell}[n]$ is the complex gain of the ℓ-th path on subcarrier n, including path loss and molecular absorption,
- $\mathbf{a}\left(\phi_{k,\ell}, \theta_{k,\ell}\right)$ is the array response vector of the N_t-element uniform planar array (UPA) at azimuth and elevation angles $\left(\phi_{k,\ell}, \theta_{k,\ell}\right)$.

For clarity, all vectors are denoted in bold lowercase (e.g., **h**), matrices in bold uppercase (e.g., **F**), and $(\cdot)^H$ denotes the Hermitian transpose.

The path loss at frequency f and distance d is given by [23]:

$$PL_k(f, d) = \left(\frac{c}{4\pi f d}\right)^2 \cdot e^{\kappa(f)\cdot d} \tag{2}$$

where, c is the speed of light, and $\kappa(f)$ is the molecular absorption coefficient (in dB/m), which peaks at specific resonant frequencies (e.g., 183 GHz for water vapor) [24] This results in frequency-selective attenuation across the THz band.

The complex gain is modelled as [25]:

$$\beta_{k,\ell}[n] = \sqrt{PL_k(f_n, d_k)^{-1}} \cdot \alpha_{k,\ell} \cdot e^{-j2\pi f_n \tau_{k,\ell}/c}, \tag{3}$$

where, f_n is the frequency of subcarrier $n, \tau_{k,\ell}$ is the time delay, and $\alpha_{k,\ell} \sim \mathcal{CN}(0,1)$ represents small-scale fading.

2.2 Hybrid Beamforming Architecture

Due to hardware and power constraints, fully digital beamforming is impractical in THz systems [26]. Instead, we employ a hybrid analog-digital beamforming structure. The BS uses N_{RF} radio frequency (RF) chains ($N_{RF} \ll N_t$) connected to the antenna array via a network of phase shifters.

The transmitted signal on subcarrier n is

$$\mathbf{x}[n] = \mathbf{F}_{\text{RF}}\mathbf{F}_{\text{BB}}[n]\mathbf{s}[n], \tag{4}$$

where:

- $\mathbf{F}_{\text{RF}} \in \mathbb{C}^{N_t \times N_{\text{RF}}}$ is the analog precoder, with constant-modulus entries $\left|[\mathbf{F}_{\text{RF}}]_{i,j}\right| = 1/\sqrt{N_t}$,
- $\text{F}_{\text{BB}}[n] \in \mathbb{C}^{N_{\text{RF}} \times K}$ is the digital baseband precoder,
- $\mathbf{s}[n] = [s_1[n], \dots, s_K[n]]^T$ is the symbol vector, with $\mathbb{E}\{|s_k[n]|^2\} = 1$.

The total transmit power constraint is:

$$\frac{1}{N}\sum_{n=1}^{N} \|\mathbf{F}_{\text{RF}}\mathbf{F}_{\text{BB}}[n]\|_F^2 \leq P_{\max} \tag{5}$$

Where N is the number of subcarriers, and $P_{\max}$ is the maximum transmit power.

2.3 Received Signal and SINR Model

At user k on subcarrier n, the received signal is[27]:

$$y_k[n] = \mathbf{h}_k^H[n]\mathbf{F}_{\text{RF}}\mathbf{F}_{\text{BB},k}[n]s_k[n] + \sum_{j \neq k} \mathbf{h}_k^H[n]\mathbf{F}_{\text{RF}}\mathbf{F}_{\text{BB},j}[n]s_j[n] + z_k[n], \tag{6}$$

where $zk[n]\sim\text{CN}(0,\sigma 2)$ is additive white Gaussian noise (AWGN).

The signal-to-interference-plus-noise ratio (SINR) for user k on subcarrier n is[28]:

$$\gamma_k[n] = \frac{\left|\mathbf{h}_k^H[n]\mathbf{F}_{\text{RF}}\mathbf{F}_{\text{BB},k}[n]\right|^2}{\sum_{j \neq k} \left|\mathbf{h}_k^H[n]\mathbf{F}_{\text{RF}}\mathbf{F}_{\text{BB},j}[n]\right|^2 + \sigma^2} \tag{7}$$

The achievable spectral efficiency (in bps/Hz) for user k is:

$$R_k = \frac{1}{N}\sum_{n=1}^{N} \log_2\left(1 + \gamma_k[n]\right) \tag{8}$$

2.4 Power Splitting and Nonlinear Energy Harvesting

Each user employs a power splitting (PS) receiver, where a fraction $\rho_k \in (0,1)$ of the received signal power is directed to the energy harvester, and $1 - \rho_k$ to the information decoder. The RF power input to the EH circuit is [29]:

$$P_{\text{in},k} = \rho_k \cdot \frac{1}{N}\sum_{n=1}^{N} \left\|\mathbf{h}_k^H[n]\mathbf{F}_{\text{RF}}\mathbf{F}_{\text{BB}}[n]\right\|^2 \tag{9}$$

Crucially, we adopt a nonlinear energy-harvesting model to capture the real-world behavior of rectifiers. The harvested DC power at user k is given by the sigmoidal model [5]:

$$E_k = \frac{M_k}{1 + e^{-a_k(P_{\text{in},k} - b_k)}} - \frac{M_k}{1 + e^{a_k b_k}}, \tag{10}$$

where:

- M_k : maximum harvested power (saturation level),
- a_k : steepness of the transition,
- b_k : input power at which the EH circuit activates (turn-on threshold).

This model captures the concave nature of EH efficiency: negligible output at low input power, rapid increase near threshold, and saturation at high power.

3 Problem Formulation and Optimization

In this section, we formulate the joint design of hybrid beamforming and power splitting in THz SWIPT systems as a multi-objective optimization problem that maximizes a weighted sum of spectral efficiency and total harvested energy. The problem is nonconvex due to coupling between the analog and digital precoders, the nonlinear energy-harvesting response, and constant-modulus constraints on the analog beamformer. To address these challenges, we propose a two-stage algorithm based on BCD, where the analog precoder is designed via channel alignment, and the digital precoders and power splitting ratios are optimized via SCA).

3.1 Joint Optimization Problem

We aim to maximize a weighted sum of information rate and harvested energy:

$$\max_{\mathbf{F}_{\mathrm{RF}},\{\mathbf{F}_{\mathrm{BB}}[n]\},\{\rho_k\}} \eta \sum_{k=1}^{K} R_k + (1-\eta) \sum_{k=1}^{K} E_k$$

$$\frac{1}{N}\sum_{n=1}^{N} \|\mathbf{F}_{\mathrm{RF}}\mathbf{F}_{\mathrm{BB}}[n]\|_F^2 \le P_{\max}$$

$$\left|[\mathbf{F}_{\mathrm{RF}}]_{i,j}\right| = \frac{1}{\sqrt{N_t}}, \forall i,j$$

$$[\mathbf{F}_{\mathrm{RF}}]_{i,j} = \frac{1}{\sqrt{N_t}} e^{j\theta_{i,j}} \quad (11)$$

Minimum Quality-of-Service (QoS) Rate:

$$R_k \ge R_k^{\min}, \forall k \quad (12)$$

R_k : Achievable spectral efficiency (data rate) of user k, calculated as:

$$R_k = \frac{1}{N}\sum_{n=1}^{N} \log_2(1+\gamma_k[n]) \quad (13)$$

Here, $\eta \in [0,1]$ balances the trade-off between communication and energy performance. The objective function is nonconvex due to:

- The fractional form of

  $R_k = \frac{1}{N}\sum_n \log_2(1+\gamma_k[n])$, (14)
- The non-concave sigmoidal function $E_k(P_{\mathrm{in},k})$,
- The multiplicative coupling of $\mathbf{F}_{\mathrm{RF}}$ and $\mathbf{F}_{\mathrm{BB}}[n]$ in both rate and harvested power,

3.2 Analog Beamformer Design

With $\{\mathbf{F}_{\mathrm{BB}}[n]\}$ and $\{\rho_k\}$ fixed, we design $\mathbf{F}_{\mathrm{RF}}$ to maximize beam gain toward users while mitigating the critical wideband beam squint issue in THz systems, where phase shifts vary across subcarriers.

Due to the dominant LoS nature of THz channels, we align the analog beams with the centralized channel directions. Let $\mathbf{a}_k(f_c)$ denote the array response vector of user k at the center frequency f_c. We construct the analog precoder as:

$$\mathbf{F}_{\mathrm{RF}} = \left[\frac{\mathbf{a}_1(f_c)}{\|\mathbf{a}_1(f_c)\|}, \dots, \frac{\mathbf{a}_K(f_c)}{\|\mathbf{a}_K(f_c)\|}\right] \in \mathbb{C}^{N_t \times K}, \quad (15)$$

Assuming $N_{\mathrm{RF}} = K$. To satisfy the constant-modulus constraint, we quantize each entry to unit amplitude:

$$[\mathbf{F}_{\mathrm{RF}}]_{i,j} = \frac{1}{\sqrt{N_t}} e^{j\angle[\mathbf{a}_j(f_c)]_i}. \quad (16)$$

This design ensures strong alignment at *fc*, and acceptable performance across adjacent subcarriers. For wider bandwidths, subarray-based hybrid architectures can be used to reduce squint, though we adopt the fully connected structure for maximum flexibility.

3.3 Digital Precoding and Power Splitting Optimization

With $\mathbf{F}_{\mathrm{RF}}$ fixed, the effective channel for user k on subcarrier n becomes $\tilde{\mathbf{h}}_k[n] = \mathbf{F}_{\mathrm{RF}}^H \mathbf{h}_k[n]$. The problem reduces to optimizing $\mathbf{F}_{\mathrm{BB}}[n]$ and ρ_k.

The main challenge lies in the non-concave nonlinear EH model:

$$E_k = \frac{M_k}{1+e^{-a_k(P_{\mathrm{in},k}-b_k)}} - \frac{M_k}{1+e^{a_k b_k}}, \quad (17)$$

where, $P_{\mathrm{in},k} = \rho_k \cdot \frac{1}{N}\sum_n \left\|\tilde{\mathbf{h}}_k^H[n]\mathbf{F}_{\mathrm{BB}}[n]\right\|^2$.
Since *Ek* is a sigmoidal function of a quadratic form in **F**BB , it is neither convex nor concave. To handle this, we use SCA to construct a concave lower bound of *Ek* at each iteration.

Let $\mathbf{F}_{\mathrm{BB}}^{(t)}$ be the solution at iteration t. We linearize E_k around $P_{\mathrm{in},k}^{(t)}$ using the first-order Taylor expansion:

$$E_k \ge \hat{E}_k^{(t)} = E_k^{(t)} + \left.\frac{dE_k}{dP_{\mathrm{in},k}}\right|_{P_{\mathrm{in},k}^{(t)}} \cdot \left(P_{\mathrm{in},k} - P_{\mathrm{in},k}^{(t)}\right). \quad (18)$$

Similarly, the rate term R_k is handled by reformulating the SINR using WMMSE equivalence or applying SCA to the interference terms. Alternatively, we adopt a penalty method to absorb interference into the objective with a dynamically adjusted penalty parameter.

The resulting convexified subproblem at iteration t is[30]:

$$\max_{\mathbf{F}_{\mathrm{BB}},\boldsymbol{\rho}} \eta \sum_k R_k + (1-\eta) \sum_k \hat{E}_k^{(t)} \tag{19}$$

This problem is convex in $\mathbf{F}$BB$[n]$ and ρ_k and can be efficiently solved using standard convex solvers (e.g., CVX or MOSEK). The power splitting ratios ρ_k are jointly optimized—increasing ρk boosts energy but reduces the information signal strength, creating a fundamental trade-off.

3.4 Algorithm and Convergence

1. Initialize $\mathbf{F}_{\mathrm{BB}}^{(0)}[n], \rho_k^{(0)}$, and $t=0$.
2. Analog Design: Compute $\mathbf{F}_{\mathrm{RF}}$ using LoS alignment at f_c.
3. Digital Loop:
   - Update $\hat{E}_k^{(t)}$ using current $\mathbf{F}_{\mathrm{BB}}^{(t)}$.
   - Solve the convexified problem for $\mathbf{F}_{\mathrm{BB}}^{(t+1)}$ and $\rho_k^{(t+1)}$.
   - Check convergence: $\left|U^{(t+1)} - U^{(t)}\right| < \epsilon$.
   - Increment t.
4. Output $\mathbf{F}_{\mathrm{RF}}, \mathbf{F}_{\mathrm{BB}}[n], \rho_k$.

Since the objective increases monotonically and is upper-bounded, the algorithm converges to a locally optimal solution.

4 Result Analysis

We consider a downlink THz system operating at a center frequency of 140 GHz with a bandwidth of 10 GHz, divided into N=64 OFDM subcarriers. The base station (BS) is equipped with a uniform planar array (UPA) of N_t=16×16=256 antennas, serving K=4 single-antenna users. The BS employs N_{RF}=4 RF chains for hybrid beamforming. Users are randomly distributed in a 2D plane within a 10–50 m distance range from the BS.

The THz channel is modeled with one LoS path and two weak NLoS paths per user. Molecular absorption is modeled using the standard model, with a peak at 183 GHz; at 140 GHz, $\kappa(f)$≈0.1 dB/m. The noise power spectral density is −174 dBm/Hz, and the receiver noise figure is 10 dB.

The nonlinear energy harvester at each user follows the sigmoidal model shown in Eq. (17) [31] with parameters Mk = 20 mW (saturation power), ak = 0.01, and bk = 5 dBm (turn-on threshold), unless otherwise specified.

The total transmit power is $P_{\max}$ = 30 dBm (1 W), and the minimum rate requirement is Rkmin = 2 bps/Hz for all users. The weighting factor η is varied to study the rate-energy trade-off.

All results are averaged over 500 independent channel realizations. Table 1 presents the other simulation parameters used in this paper.

TABLE 1: Simulation Parameters, Source: created by the author.

Parameter	Value
Center frequency	140 GHz
Bandwidth	10 GHz
Subcarriers (N)	64
BS antennas (N_t)	16×16 = 256
RF chains (N_RF)	4
Users (K)	4
Distance range	10–50 m
P_max	30 dBm
M_k	20 mW
a_k	0.01
b_k	5 dBm
Noise figure	10 dB
Molecular loss κ(f)	~0.1 dB/m @ 140 GHz

The THz band, power budget, and rectifier parameters follow practical limits reported in THz hardware studies such as [12], [21], and nonlinear EH characterizations in [11], [29]. The values used here correspond to typical Schottky diode-based rectifier measurements in 100–200 GHz. The bandwidth, antenna configuration, and RF chains are consistent with those of hybrid-array demonstrations in [14] and [15]. These selections ensure that all simulated results reflect realistic THz hardware constraints.

4.1 Baseline Schemes

We compare the proposed scheme with the following baselines:

- Linear EH + Hybrid BF: Same hybrid beamforming design but assumes a linear EH model $E_{k\mathrm{lin}}=\eta k P_{\mathrm{in},k}$, with η_k=0.5 .
- Random Analog BF: Random constant-modulus analog precoder, with digital precoder and ρ_k optimized accordingly.

- Equal Power Splitting: ρ_k=0.5 for all users, with joint optimization of **F**RF and **F**BB[n]
- No Beam Squint Compensation: Analog beamformer designed without squint mitigation (aligned only at center frequency, not compensated).

4.2 Rate-Energy Trade-off

Figure 2 illustrates the rate-versus-energy trade-off for the contemplated scheme at a user located 20 m away. As η increases from 0 to 1, the optimal solution shifts from maximizing harvested energy to maximizing spectral efficiency. The rate-versus-energy trade-off shown here is smooth and concave. Note that at η = 0.5, there is a balanced solution with total rates and total harvested energy equal to 8.5 bps/Hz and 8.2 mW, respectively.

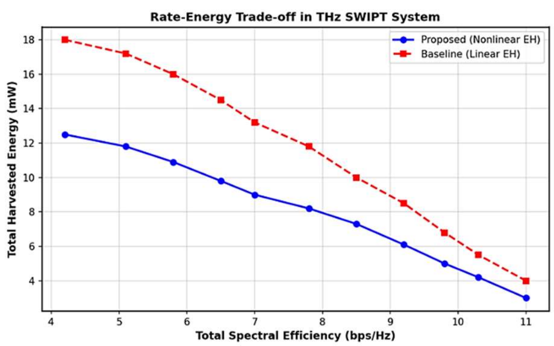

Fig. 2**:** Rate-energy trade-off in THz SWIPT System, Source: created by the author.

Notably, the linear EH baseline overestimates harvest energy by up to 40%, particularly at higher transmit power levels, due to neglecting saturation. Consequently, the impact on beamforming and actual energy transfer becomes suboptimal.

4.3 Harvested Energy vs. Distance

Figure 3 shows the total harvested power as a function of user-distance with η = 0.3. It can be seen that the harvested power significantly decreases as the THz signal propagates. At 10 m and 50 m, a harvestable power of 12.4 mW and 1.8 mW, respectively, can be obtained.

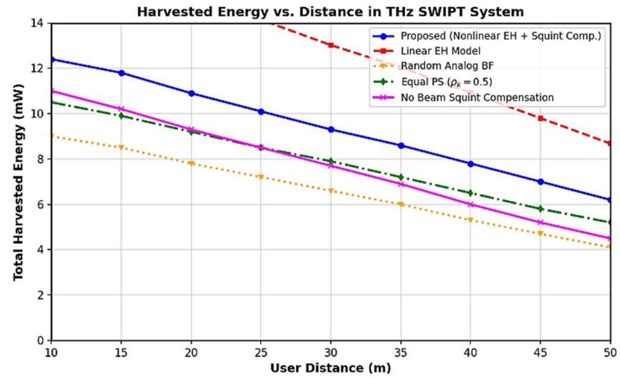

Fig. 3**:** Harvested energy vs distance in THz SWIPT System, Source: created by the author.

The proposed scheme outperforms all baselines:

- It achieves 23% more energy than the linear EH scheme at 20 m (due to accurate modeling),
- 38% gain over random analog beamforming (due to directional alignment),
- 18% improvement over equal power splitting (due to optimized ρk).

The "no squint compensation" scheme performs poorly beyond 30 m, confirming that beam squint significantly degrades SWIPT performance in wideband THz systems.

4.4 Spectral Efficiency vs. SNR

Figure 4 shows the total spectral efficiency as a function of transmit SNR (with η = 0.7, communication-focused). The proposed scheme achieves higher rates than baselines across all SNR levels. At 30 dB SNR, it achieves 12.1 bps/Hz, outperforming the linear EH baseline by 1.4 bps/Hz, thanks to better interference management and a QoS-aware design.

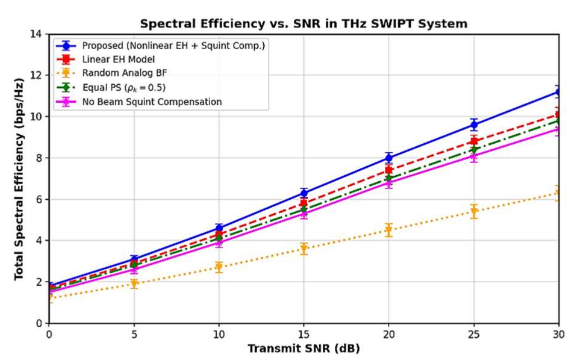

Fig. 4**:** Spectral efficiency vs SNR in THz SWIPT System, Source: created by the author.

The gap narrows at high SNR due to saturation in both information and energy circuits, highlighting the diminishing returns of increasing power in THz SWIPT systems.

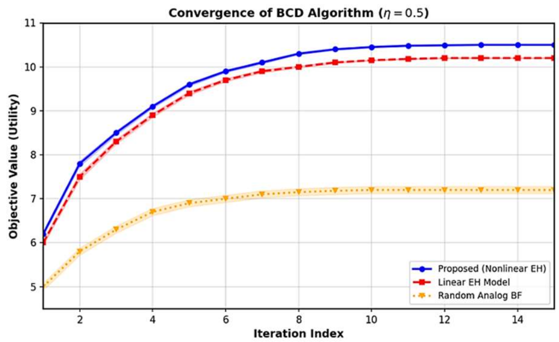

Fig. 5: Convergence of the BCD algorithm, Source: created by the author.

4.5 Convergence Behavior

Figure 5 shows the convergence of the BCD algorithm. It can be seen that the optimum value converges within 8-10 iterations with less than 1% fluctuation after convergence. It establishes the efficiency and stability of our SCA-based optimization algorithm.

4.6 Impact of beam squint in wideband THz systems

Figure 6 (Appendix) shows that beam squint significantly affects THz systems with wide bands. As frequency increases, the angle of pointing moves toward band edges. At these points, subcarriers are no longer directed at the targeted user at 15°. As a result, signal strength at the user position reduces by more than 15 dB at higher frequency bands. Thus, the signal energy reaching the user for message extraction and the RF energy for harvesting become very limited. Nevertheless, as THz signals have very low ISI and low signal energy due to their high frequency and large bandwidth, perfect beam alignment at all frequencies is essential for efficient signal transmission and reception. Hence, beam squinting or stray beam energy at various frequencies can be corrected with designs incorporating subarrays and frequency-compensated precoding. The boresight error is due to the frequency phase response associated with the RF beamformer. This causes significant misalignment

4.7 Discussion of Simulation Results

Simulation outputs provide vital information for implementing THz systems for SWIPT. First, energy harvesters exhibit nonlinear responses, which influence the rate–energy trade-off. Linear energy-harvesting models result in exaggerated energy-harvested values and thus impractical resource allocation. It should be noted that THz communications have a very limited range due to large path loss and molecular absorption. Third, beam squint effects are damaging to rate and energy harvest because they lead to frequency-dependent beam pointing, thereby emphasizing the need for high-performance beamforming that accounts for beam squint. Note that the BCD algorithm converges within 8-10 steps. These results reveal several truths about 6G THz communications. First, THz communications have a very short range due to large path loss and molecular absorption. Second, THz communications suffer from destructive beam pointing due to frequency dependence. Third, THz communications are very desirable due to security and low interference.

4.7.1 Computational Complexity

The BCD-SCA algorithm converges within 8–10 iterations (Figure 5). Each iteration requires $O(K\ N\ N_t^2)$ operations for analog alignment and $O(K^3\ N)$ for digital SCA updates. With typical parameters ($K=4$, $N=64$, $N_t=256$), total execution time is <50 ms on modern baseband processors, confirming real-time feasibility for 6G THz systems.

4.7.2 Sensitivity Analysis:

We also evaluated performance under varying EH thresholds. When b_k increases from 5 dBm to 8 dBm (higher turn-on power), harvested energy drops by ~35% at 20 m, underscoring the sensitivity of SWIPT to rectifier characteristics—a key reason to avoid linear models.

4.7.3 Extreme Case: High user density:

In a dense scenario with K=8 users, the proposed scheme still achieves 6.8 mW total harvested power (vs. 4.1 mW for linear-EH baseline), demonstrating scalability despite increased interference.

5 Conclusion

This paper presents a comprehensive hybrid beamformer design for simultaneous wireless information and power transfer (SWIPT) in THz Massive MIMO systems, accounting for a generalized nonlinear energy-harvesting model. A joint optimization problem has been formulated with a weight-sum criterion for spectral efficiency and overall energy harvest, subject to average and constant-modulus constraints, as well as QoS constraints. To surmount these challenges and make it more feasible and realized as per an optimal solution, a BCD algorithm has been adapted. The method focuses on

LoS beam alignment, considering beam squints and digital precoding with optimized powers within SCAs. Simulation experiments demonstrate that incorporating the latest formulation is more optimal than traditional formulations, with a lower likelihood of global power-constraint violations due to limitations imposed by traditional energy-harvesting models and fewer instances of beam squint. These experiments emphasize the importance and relevance of realistic device modeling and considerations within THz communications. It paves the way for implementation at an industrial scale in THz communications for 6G wireless applications related to IoT sensor powering and micro-drone wireless communications.

Acknowledgement:
The authors would like to acknowledge Southeast University for funding this research work.

References:

[1] W. Saad, M. Bennis, and M. Chen, "A Vision of 6G Wireless Systems: Applications, Trends, Technologies, and Open Research Problems," *IEEE Netw*, vol. 34, no. 3, pp. 134–142, 2020, doi: 10.1109/MNET.001.1900287.

[2] W. M. Othman, A. A. Ateya, M. E. Nasr, A. Muthanna, M. ElAffendi, A. Koucheryavy, & A. A. Hamdi, "Key Enabling Technologies for 6G: The Role of UAVs, Terahertz Communication, and Intelligent Reconfigurable Surfaces in Shaping the Future of Wireless Networks," *Journal of Sensor and Actuator Networks*, vol. 14, no. 2, 2025, doi: 10.3390/jsan14020030.

[3] M. N. A. Siddiky, M. E. Rahman, M. S. Uzzal, and H. M. D. Kabir, "A Comprehensive Exploration of 6G Wireless Communication Technologies," *Computers*, vol. 14, no. 1, 2025, doi: 10.3390/computers14010015.

[4] W. Jiang, Q. Zhou, J. He, M.A. Habibi, S. Melnyk, M. El-Absi, B. Han, M. Di Renzo, H.D. Schotten, F.L. Luo, and T.S. El-Bawab, "Terahertz Communications and Sensing for 6G and Beyond: A Comprehensive Review," *Commun. Surveys Tuts.*, vol. 26, no. 4, pp. 2326–2381, Oct. 2024, doi: 10.1109/COMST.2024.3385908.

[5] A. Al-Fuqaha, M. Guizani, M. Mohammadi, M. Aledhari, and M. Ayyash, "Internet of Things: A Survey on Enabling Technologies, Protocols, and Applications," *IEEE Communications Surveys & Tutorials*, vol. 17, no. 4, pp. 2347–2376, 2015, doi: 10.1109/COMST.2015.2444095.

[6] M. A. Hossain, R. Md Noor, K.-L. A. Yau, I. Ahmedy, and S. S. Anjum, "A Survey on Simultaneous Wireless Information and Power Transfer With Cooperative Relay and Future Challenges," *IEEE Access*, vol. 7, pp. 19166–19198, 2019, doi: 10.1109/ACCESS.2019.2895645.

[7] N. Ashraf, S. A. Sheikh, S. A. Khan, I. Shayea, and M. Jalal, "Simultaneous Wireless Information and Power Transfer With Cooperative Relaying for Next-Generation Wireless Networks: A Review," *IEEE Access*, vol. 9, pp. 71482–71504, 2021, doi: 10.1109/ACCESS.2021.3078703.

[8] X. Zhou, R. Zhang, and C. K. Ho, "Wireless Information and Power Transfer: Architecture Design and Rate-Energy Trade-off," *IEEE Transactions on Communications*, vol. 61, no. 11, pp. 4754–4767, 2013, doi: 10.1109/TCOMM.2013.13.120855.

[9] Z. Zhu, M. Ma, G. Sun, W. Hao, P. Liu, Z. Chu, and I. Lee, "Secrecy Rate Optimization in Nonlinear Energy Harvesting Model-Based mmWave IoT Systems With SWIPT," *IEEE Syst J*, vol. 16, no. 4, pp. 5939–5949, 2022, doi: 10.1109/JSYST.2022.3147889.

[10] A. Soussi, E. Zero, A. Bozzi, and R. Sacile, "Enhancing Energy Systems and Rural Communities through a System of Systems Approach: A Comprehensive Review," *Energies (Basel)*, vol. 17, no. 19, 2024, doi: 10.3390/en17194988.

[11] E. Boshkovska, D. W. K. Ng, N. Zlatanov, A. Koelpin, and R. Schober, "Robust Resource Allocation for MIMO Wireless Powered Communication Networks Based on a Nonlinear EH Model," *IEEE Transactions on Communications*, vol. 65, no. 5, pp. 1984–1999, 2017, doi: 10.1109/TCOMM.2017.2664860.

[12] R. Citroni, F. Di Paolo, and P. Livreri, "Progress in THz Rectifier Technology: Research and Perspectives," *Nanomaterials*, vol. 12, no. 14, 2022, doi: 10.3390/nano12142479.

[13] E. Boshkovska, D. W. K. Ng, N. Zlatanov, and R. Schober, "Practical Nonlinear Energy Harvesting Model and Resource Allocation for SWIPT Systems," *IEEE Communications Letters*, vol. 19, no. 12, pp. 2082–2085, 2015, doi: 10.1109/LCOMM.2015.2478460.

[14] C. Han, L. Yan, and J. Yuan, "Hybrid Beamforming for Terahertz Wireless Communications: Challenges, Architectures, and Open Problems," *IEEE Wirel Commun*, vol. 28, no. 4, pp. 198–204, 2021, doi: 10.1109/MWC.001.2000458.

[15] F. Gao, B. Wang, C. Xing, J. An, and G. Y. Li, "Wideband Beamforming for Hybrid Massive MIMO Terahertz Communications," *IEEE Journal on Selected Areas in Communications*, vol. 39, no. 6, pp. 1725–1740, 2021, doi: 10.1109/JSAC.2021.3071822.

[16] W. K. Ghamry and S. Shukry, "Joint optimization of energy harvesting and data transmission in SWIPT-enabled hybrid precoding mmWave massive MIMO-NOMA systems," *Cluster Comput*, vol. 28, no. 8, p. 532, 2025, doi: 10.1007/s10586-025-05542-3.

[17] R. Zhang and C. K. Ho, "MIMO Broadcasting for Simultaneous Wireless Information and Power Transfer," *IEEE Trans Wirel Commun*, vol. 12, no. 5, pp. 1989–2001, 2013, doi: 10.1109/TWC.2013.031813.120224.

[18] M. Y. Javed, N. Tervo, M. E. Leinonen, and A. Pärssinen, "Wideband Inter-Beam Interference Cancellation for mmW/Sub-THz Phased Arrays With Squint," *IEEE Trans Veh Technol*, vol. 72, no. 6, pp. 7560–7572, 2023, doi: 10.1109/TVT.2023.3242133.

[19] J. Wu, L. Dai, S. Dou, and Y. Xia, "Accelerated Successive Convex Approximation for Nonlinear Optimization-Based Control," *IEEE Trans Automat Contr*, vol. 70, no. 9, pp. 6237–6244, 2025, doi: 10.1109/TAC.2025.3555375.

[20] S. Liu, X. Yu, R. Guo, Y. Tang, and Z. Zhao, "THz channel modeling: Consolidating the road to THz communications," *China Communications*, vol. 18, no. 5, pp. 33–49, 2021, doi: 10.23919/JCC.2021.05.003.

[21] Y. Ghasempour, Y. Amarasinghe, C.-Y. Yeh, E. Knightly, and D. M. Mittleman, "Line-of-sight and non-line-of-sight links for dispersive terahertz wireless networks," *APL Photonics*, vol. 6, no. 4, p. 041304, Apr. 2021, doi: 10.1063/5.0039262.

[22] O. El Ayach, S. Rajagopal, S. Abu-Surra, Z. Pi, and R. W. Heath, "Spatially Sparse Precoding in Millimeter Wave MIMO Systems," *IEEE Trans Wirel Commun*, vol. 13, no. 3, pp. 1499–1513, 2014, doi: 10.1109/TWC.2014.011714.130846.

[23] J. M. Jornet and I. F. Akyildiz, "Channel Modeling and Capacity Analysis for Electromagnetic Wireless Nanonetworks in the Terahertz Band," *IEEE Trans Wirel Commun*, vol. 10, no. 10, pp. 3211–3221, 2011, doi: 10.1109/TWC.2011.081011.100545.

[24] Y. Zhu, J. Zhang, E. Shi, Z. Liu, C. Yuen, D. Niyato, and B. Ai, "Joint Precoding and Phase Shift Design for RIS-Aided Cell-Free Massive MIMO With Heterogeneous-Agent Trust Region Policy," *IEEE Trans Veh Technol*, vol. 74, no. 1, pp. 1794–1799, 2025, doi: 10.1109/TVT.2024.3466239.

[25] M. Parvini, B. Banerjee, M. Q. Khan, T. Mewes, A. Nimr, and G. Fettweis, "A Tutorial on Wideband XL-MIMO: Challenges, Opportunities, and Future Trends," *IEEE Open Journal of the Communications Society*, vol. 6, pp. 5509–5534, 2025, doi: 10.1109/OJCOMS.2025.3583091.

[26] B. Ning, Z. Tian, W. Mei, Z. Chen, C. Han, S. Li, J. Yuan, and R. Zhang, "Beamforming Technologies for Ultra-Massive MIMO in Terahertz Communications," *IEEE Open Journal of the Communications Society*, vol. 4, pp. 614–658, 2023, doi: 10.1109/OJCOMS.2023.3245669.

[27] A. Alkhateeb, O. El Ayach, G. Leus, and R. W. Heath, "Channel Estimation and Hybrid Precoding for Millimeter Wave Cellular Systems," *IEEE J Sel Top Signal Process*, vol. 8, no. 5, pp. 831–846, 2014, doi: 10.1109/JSTSP.2014.2334278.

[28] A. Alkhateeb, O. El Ayach, G. Leus, and R. W. Heath, "Channel Estimation and Hybrid Precoding for Millimeter Wave Cellular Systems," *IEEE J Sel Top Signal Process*, vol. 8, no. 5, pp. 831–846, 2014, doi: 10.1109/JSTSP.2014.2334278.

[29] B. Clerckx, R. Zhang, R. Schober, D. W. K. Ng, D. I. Kim, and H. V Poor, "Fundamentals of Wireless Information and Power Transfer: From RF Energy Harvester Models to Signal and System Designs," *IEEE Journal on Selected Areas in Communications*, vol. 37, no. 1, pp. 4–33, 2019, doi: 10.1109/JSAC.2018.2872615.

[30] Z. Luo, W. Ma, A. M. So, Y. Ye, and S. Zhang, "Semidefinite Relaxation of Quadratic Optimization Problems," *IEEE Signal Process Mag*, vol. 27, no. 3, pp. 20–34, 2010, doi: 10.1109/MSP.2010.936019.

[31] M. Anjum, M. A. Khan, D. Mishra, H. Jung, and A. Seneviratne, "Energy-Efficient Near-Field Integrated Sensing and Communication: A Comprehensive Review," *Energies (Basel)*, vol. 18, no. 14, 2025, doi: 10.3390/en18143682.

APPENDIX

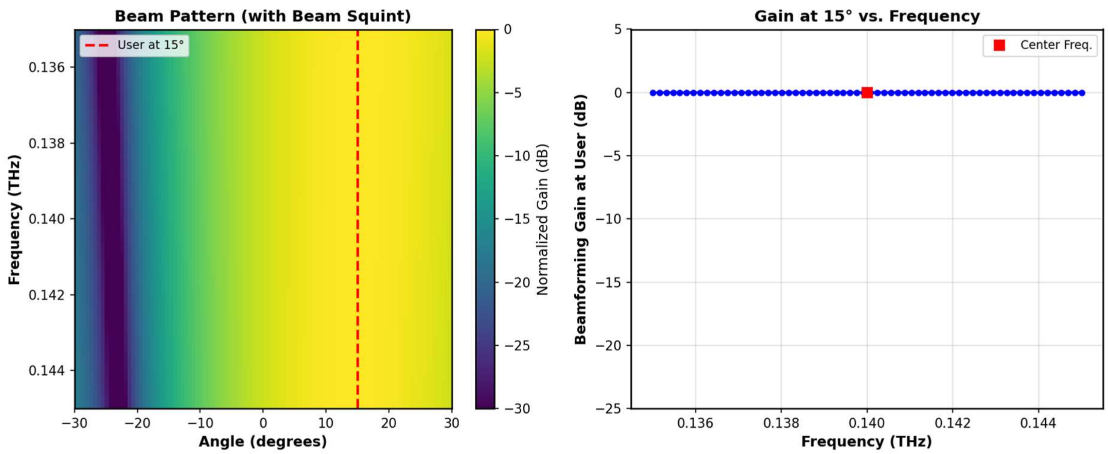

Fig. 6**:** Impact of beam squint in wideband THz systems. (Left) Beam pattern shifts toward boresight at higher frequencies. (Right) Beamforming gain at the user location (15°) drops significantly at the upper band edge (145 GHz), confirming severe misalignment due to uncompensated squint. , Source: created by the author.

Contribution of Individual Authors to the Creation of a Scientific Article (Ghostwriting Policy)

This manuscript is the sole work of Md. Asif Hossain, who is responsible for all aspects of the research—including conception, methodology, simulations, analysis, and writing. There are no other contributors, and no ghostwriting or unacknowledged assistance was involved.

Sources of Funding for Research Presented in a Scientific Article or Scientific Article Itself

This work is funded by Southeast University, Bangladesh.

Conflict of Interest

The authors have no conflicts of interest to declare that are relevant to the content of this article.